

## Automatic Landslide Inventory Generation Using Deep Learning

Lu-Yu Ju<sup>1</sup>, Te Xiao<sup>2</sup> and Limin Zhang<sup>3</sup>

<sup>1</sup>Department of Civil and Environment Engineering, The Hong Kong University of Science and Technology, Hong Kong SAR, China. E-mail: lju@connect.ust.hk

<sup>2</sup>Department of Civil and Environment Engineering, The Hong Kong University of Science and Technology, Hong Kong SAR, China. E-mail: xiaote@ust.hk

<sup>3</sup>Department of Civil and Environment Engineering, The Hong Kong University of Science and Technology, Hong Kong SAR, China. E-mail: cezhangl@ust.hk

**Abstract:** With the rapid development of deep learning algorithms and easier access to remote sensing images, deep learning-based landslide identification using remote sensing images becomes possible. Pan-sharpening techniques are often adopted to fuse low-resolution multispectral images and high-resolution panchromatic images. This paper combines the deep learning and pan-sharpening techniques to enhance landslide identification results and compares the performance of four pan-sharpening techniques and two deep learning models. Eventually, morphological image processing is adopted to segment landslide clusters into individual landslides and form a basic landslide inventory. A case study of East Sai Kung, Hong Kong, shows that pan-sharpening techniques improve landslide identification accuracy and U-Net model with Brovey sharpening perform the best in this study.

Keywords: Landslide inventory; landslide identification; remote sensing; pan-sharpening; deep learning.

### 1 Introduction

Preparation of landslide inventories is a primary task in quantitative landslide risk assessment and mitigation (Guzzetti et al. 2012; Fan et al. 2018; Xiao et al. 2022). Conventionally, landslide inventories are often produced based on geological field surveys or visual interpretation of remote sensing images (Nichol and Wong 2005). These methods are labor-intensive and time-consuming, especially when a large area is covered. A well-known landslide inventory in Hong Kong is ENTLI (Enhanced Natural Terrain Landslide Inventory) (Dias et al. 2009), which consists of more than 111,000 historical natural terrain landslides up to 2019.

Emerging deep learning techniques have been applied to facilitate landslide identification with increasingly accessible remote sensing images (Ghorbanzadeh et al. 2019; Lei et al. 2019; Wang et al., 2020; Zhang et al. 2020; Su et al. 2021). Although the efficiency and accuracy of landslide identification can be significantly improved using deep learning, most of them adopts a semantic segmentation strategy with representatives such as U-Net (Ronneberger et al. 2015), SegNet (Badrinarayanan et al. 2016) and DeepLab (Chen et al. 2018). This semantic segmentation strategy does separate landslides and non-landslides in the images (i.e., labeling landslides as 1 and non-landslides as 0), but cannot differentiate between different landslides (i.e., labeling different landslides as different numbers). The latter is particularly critical to characterize the feature of each landslide to generate a landslide inventory.

On the other hand, remote sensing images usually include multispectral images and panchromatic images. Compared with panchromatic images, multispectral images contain color information of ground objects but with lower spatial resolution. Pan-sharpening techniques (Zhang and Mishra 2012) are widely adopted to fuse the low-resolution multispectral image and the high-resolution panchromatic image at the same location to produce an updated high-resolution multispectral image. It is expected that the accuracy of landslide identification can be improved based on the pan-sharpened image.

This study aims to automatically generate a landslide inventory for Hong Kong using deep learning techniques. Pan-sharpening is first applied to obtain high-resolution multispectral images, based on which deep learning is then used for landslide identification. Morphological image processing is afterwards adopted to segment different landslide instances and form a basic landslide inventory. A case study of East Sai Kung, Hong Kong is investigated to demonstrate the capacity of the proposed framework.

### 2 Automatic landslide inventory generation

This study proposes an automatic landslide inventory generation framework consisting of three steps; namely image enhancement using pan-sharpening, landslide identification using deep learning, and landslide segmentation using morphological image processing. Once the boundary of each landslide is determined, several geometry records of each landslide, such as the crown, trace, and area of landslide, like those included in ENTLI, can be quantified to form a basic landslide inventory.

## 2.1 Image enhancement using pan-sharpening

The pan-sharpening step aims to fuse the low-resolution multispectral image and high-resolution panchromatic image at the same location to produce an updated high-resolution multispectral image. Four pan-sharpening techniques, i.e., Brovey, principal component (PC), color normalized (CN), and Gram-Schmidt (GS) spectral sharpening algorithms, are adopted to compare their performances.

The Brovey method sharpens the images by multiplying each band of the multispectral image with a ratio of the high-resolution data to the sum of the color bands. The color bands of multispectral image are resampled to high-resolution pixel size using interpolation techniques.

The principal component method first transforms multispectral bands to principal components and an inverse principal component transformation is then performed after replacing the first principal component by high-resolution panchromatic image.

The color normalized method is an extension of Brovey algorithm, in which only the multispectral bands falling within spectral range of panchromatic image are sharpened.

The Gram-Schmidt method first reproduces a low-resolution panchromatic band from the multispectral bands, followed by a Gram-Schmidt transform on the reproduced low-resolution panchromatic band and multispectral bands (panchromatic band is taken as the first band). By taking the high-resolution panchromatic band as the first band of the Gram-Schmidt transformed bands, an inverse Gram-Schmidt transform is applied to construct the pan-sharpened multispectral bands.

## 2.2 Landslide identification using deep learning

Two candidate semantic segmentation models, namely U-Net and DeepLab, are applied for landslide identification. Their modified network structures are shown in Figure. 1. The U-Net is a 58-layer network structure modified from a fully convolutional network. The structure maintains the encoding process of the fully convolutional network to extract image features. It combines the low-level features obtained in the encoding process with the upsampling results to achieve more accurate positioning and prediction in the decoding process. A large number of feature channels are maintained during decoding (e.g., 512 channels are produced after first upsampling process), which enables the model to transmit background information to improve its accuracy.

Figure. 1(b) shows a modified network structure from DeepLabV3+. The model adopts the strategy of spatial pyramid pooling to ensure that multi-scale contextual information can be learned. An encoder-decoder strategy similar to U-Net is adopted to capture sharper object boundaries. Different to U-Net, only the features of one stage are fused in the decoding process. The results obtained from the encoding process are first upsampled by the bilinear sampling method with a factor of 4, and then concatenated with the corresponding low-level features. In this study, the network backbone of DeepLabV3+ is Res-Net18 with 100 layers.

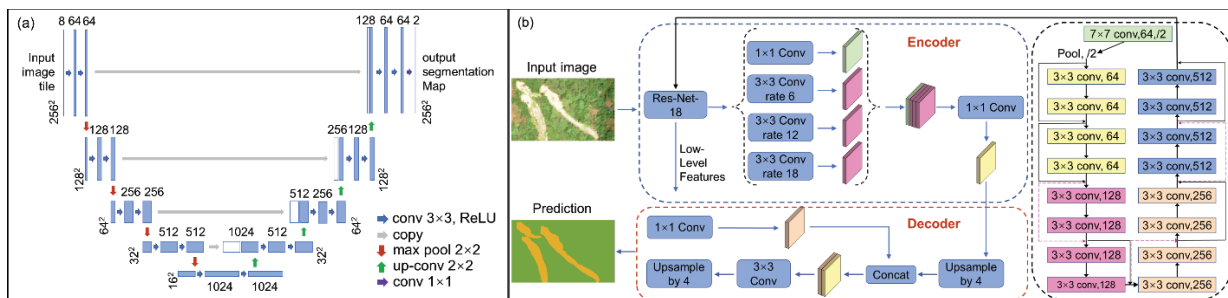


Figure 1. Architecture of modified (a) U-Net and (b) DeepLabV3+ for landslide identification.

## 2.3 Landslide segmentation using morphological image processing

The identification result of semantic segmentation is a binary image with 1 and 0 for landslide and background, respectively. The identified landslide instances are mixed with the same number, making it difficult to analyze the landslide attributes. This study introduces a morphological image processing-based landslide segmentation step as a post-processing step of deep learning to separate the identified landslides, as follows:

(a) The binary image is first eroded to remove undesired cluster pixels with small areas, according to a flat morphological structuring element (e.g., a square structuring element with width of 8 pixels).

(b) The image is then dilated with the same morphological structuring element to merge pixels separated during the erosion operation.

(c) All connected components in the binary image are identified as independent landslides and the boundaries are extracted as landslide polygons.

(d) Those connected components are further skeletonized to polylines to obtain landslide traces and the end points with higher terrain elevation are identified as landslide crowns.



(e) The area and runout distance of each landslide can be estimated, together with the crown (point), trace (polyline) and impact area (polygon) of landslide, to form a basic landslide inventory, similar to the information contained in ENTLI.

### 3 Case study of East Sai Kung

The East Sai Kung, Hong Kong (Figure. 2(a)) is taken as a case study. During the rainy season of 2014 and 2016, a large number of landslides occurred in this area, as observed from the WorldView-2 satellite images, among which the resolutions of the multispectral image (Figure. 2(a)) and the panchromatic image (Figure. 2(b)) are 1.92 m and 0.48 m, respectively. As shown in Figure. 2(a), landslides in two red rectangular regions are selected for training and testing the deep learning-based landslide identification models.

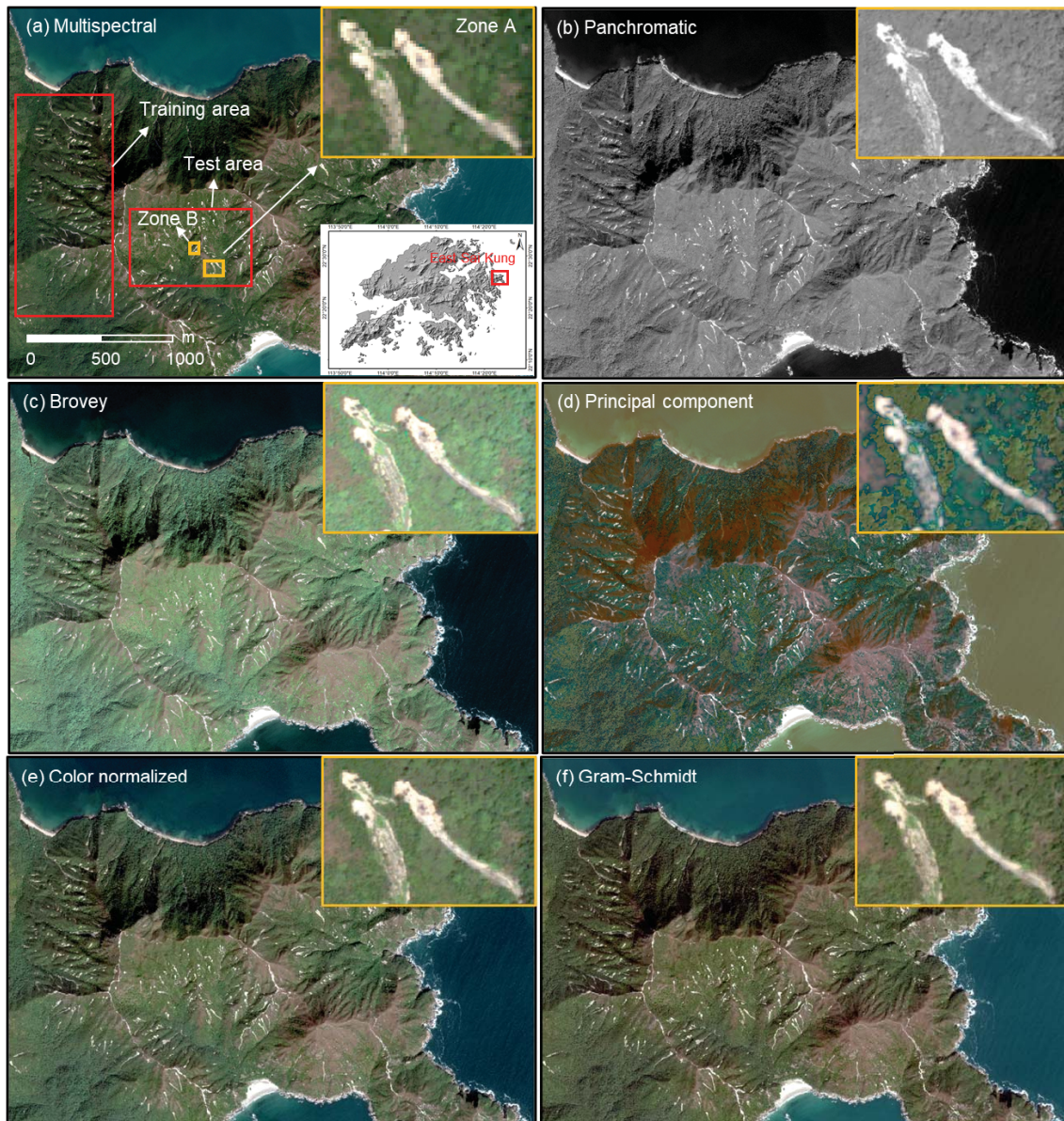


**Figure 2.** Satellite images of East Sai Kung: (a) multispectral image; (b) panchromatic image; and pan-sharpened images using (c) Brovey, (d) principal component, (e) color normalized and (f) Gram-Schmidt methods.

Figure 2(c)-(f) provide the sharpened 0.48m-resolution multispectral images using four pan-sharpening methods. The results of color normalized and Gram-Schmidt methods appear to be more satisfactory. The tone of the fused image based on principal component method changes significantly, which is caused by the high concentration of the first principal component information. The pan-sharpened images have higher resolution than the multispectral image and more distinct features than the panchromatic image. The contrast difference between landslides and non-landslides is more obvious, which facilitates landslide labeling in machine learning.



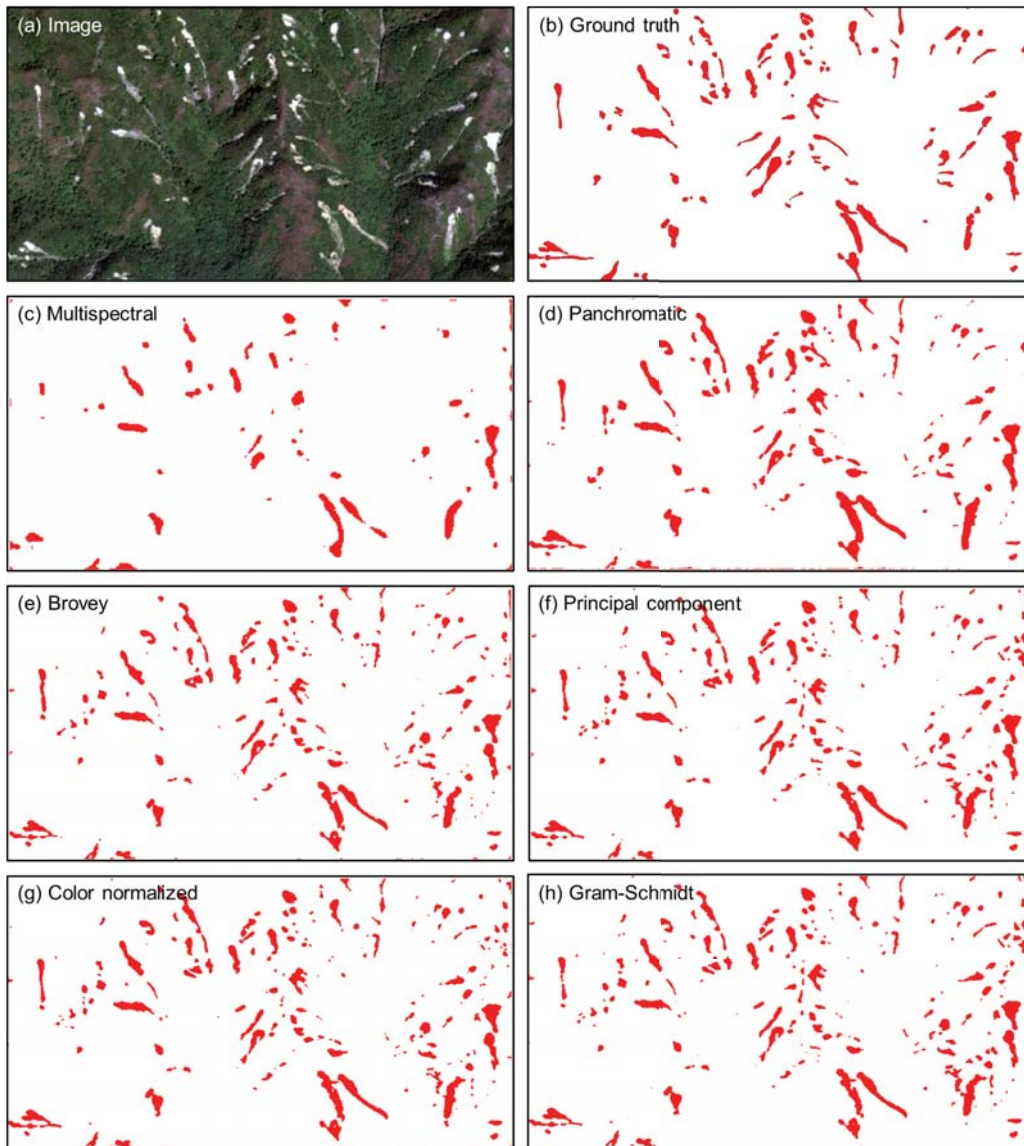


**Figure 3.** Landslide identification results of test dataset using U-Net: (a) satellite image; (b) ground truth; and identified landslides based on (c) multispectral image; (d) panchromatic image; and pan-sharpened images using (e) Brovey; (f) principal component; (g) color normalized; (h) Gram-Schmidt methods.

### 3.1 Model training and validation

Based on the training images in the aforementioned multispectral image, panchromatic image and pan-sharpened images, twelve landslide identification models are trained using U-Net and DeepLabV3+, respectively. Figure. 3 presents the identification results of the test zone using the U-Net model. Figure. 3(b) is the landslide ground truth depicted according to satellite images and serves as a benchmark to evaluate the landslide identification results. With the low-resolution multispectral image, a large number of landslides cannot be identified. Regarding the high-resolution panchromatic image, nearly all landslides can be identified but the identified boundaries are much larger than those of the ground truth. The identification results based on the sharpened images are similar and closer to the real landslide boundaries, indicating that the pan-sharpening enhanced deep learning can improve landslide identification work.

Figure. 4 compares a quantitative evaluation index, IoU, for different combinations of pan-sharpening methods and deep learning models, which is defined as:

$$\text{IoU} = \text{TP} / (\text{TP} + \text{FP} + \text{FN}) \quad (1)$$

where TP is the number of true positive predictions (the prediction is landslide and consistent with the ground truth); FP is the number of false positive predictions (the prediction is landslide but the ground truth is not); FN is the number of false negative predictions (the prediction is not landslide and the ground truth is not either); and FN is the number of false negative predictions.

As shown in Figure. 4, U-Net has a better performance than the DeepLabV3+ in this study. When using the DeepLabV3+ model, the IoU values are only 0.477 and 0.531, respectively, if the multispectral image and the panchromatic image are used. When the sharpened images are adopted for landslide identification, the

identification accuracy can be significantly improved and the highest IoU can reach 0.624 with Gram-Schmidt pan-sharpening. When the U-Net model is applied, the Brovey pan-sharpening is the best with IoU of 0.657. The U-Net model with Brovey sharpening is finally taken as the best choice for analyzing landslide attributes.

Applying the morphological image processing techniques, the number and area of segmented landslides in the testing region are 199 and 23,042 m<sup>2</sup>, respectively, slightly larger than the actual number (i.e., 110) and area (i.e., 19,799 m<sup>2</sup>). This may be because that some landslides are identified as multiple small landslides due to recovery of vegetation and the identified boundary is a little larger than the interpreted boundary. Figure 5 gives an example of one landslide in zone B as shown in Figure 2(a). The identified landslide crown, trace and boundary is consistent with the ground truth extracted from ENTLI.

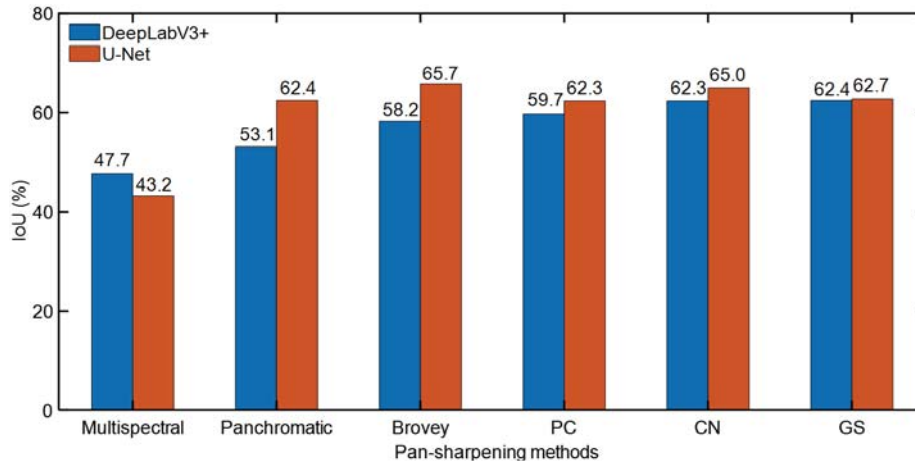


Figure 4. IoU values for different combinations of pan-sharpening methods and deep learning models.

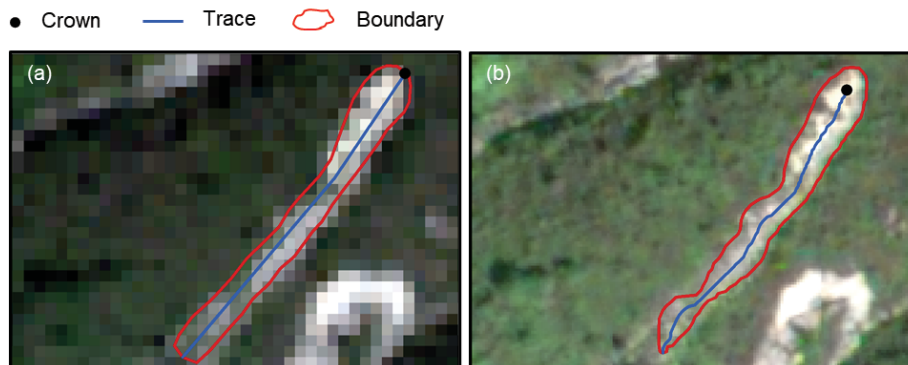


Figure 5. A landslide example: (a) ground truth; (b) identified results.

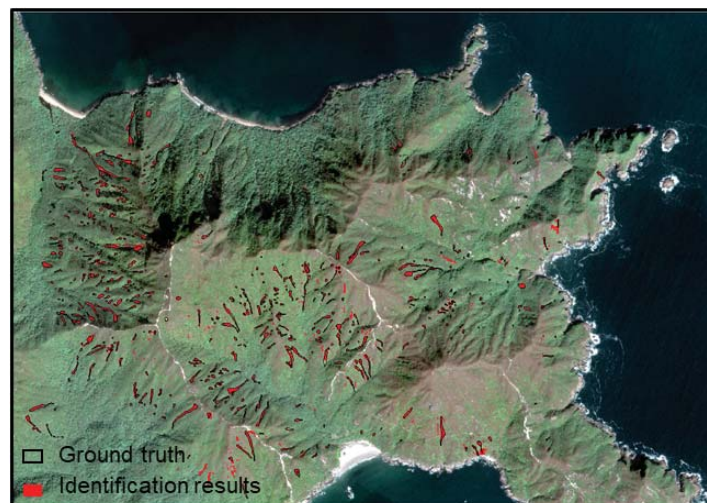


Figure 6. Landslide inventory of East Sai Kung.

### 3.2 Landslide inventory of East Sai Kung

Taking the U-Net model with Brovey sharpening, a landslide inventory in East Sai Kung is automatically generated. As shown in Figure 6, the identified landslides agree well with the ground truth in this area. Applying

the morphological image processing technique for landslide segmentation, the identified landslides can be separated to extract the landslide crowns and traces with attributes such as the length of trace and impact area. A total of 999 landslides are identified with a total area of 121,309 m<sup>2</sup>. The total area is close to the true value (i.e., 121,719 m<sup>2</sup>), while the number identified is larger than that in ENTLI (i.e., 589). Again, this is because some landslides are identified as several small ones due to recovery of vegetation in the middle of some landslides. The ENTLI has corrected this issue with engineering judgement. More efforts should be paid in the future to automatically combine these small and nearly connected landslide areas into one complete landslide.

#### 4 Conclusions

This study proposes an automatic landslide inventory generation method consisting of three steps, namely image enhancement using pan-sharpening, landslide identification using deep learning, and landslide segmentation using morphological image processing. A case study of East Sai Kung, Hong Kong is investigated to demonstrate the capacity of the proposed framework.

The pan-sharpening techniques improve the accuracy of deep learning-based landslide identification. When using the DeepLabV3+ model, the Gram-Schmidt sharpening method is the best with IoU of 0.624; when the U-Net model is applied, the Brovey method is the best with IoU of 0.657. The U-Net model has a better model performance than the DeepLabV3+ model in this study. Eventually, a landslide inventory with 999 landslides covering 121,719 m<sup>2</sup> area is established for East Sai Kung.

#### Acknowledgments

This work was supported by the Research Grants Council of the Hong Kong SAR Government (Project Nos. 16205719, 16203720 and AoE/E-603/18). The authors would like to thank the Geotechnical Engineering Office of the Civil Engineering and Development Department, the Government of the Hong Kong Special Administrative Region, for providing the satellite images.

#### References

- Badrinarayanan, V., Kendall, A., and Cipolla, R. (2017). Segnet: A deep convolutional encoder-decoder architecture for image segmentation. *IEEE Transactions on Pattern Analysis and Machine Intelligence*, 39(12), 2481-2495.
- Chen, L.C., Zhu, Y., Papandreou, G., Schroff, F., and Adam, H. (2018). Encoder-decoder with atrous separable convolution for semantic image segmentation. *Proceedings of the European Conference on Computer Vision*, 801-818.
- Dias, A., Hart, J.R., and Fung, E.K.S. (2009). The enhanced natural terrain landslide inventory. Proceedings of 17th Annual Conference of the Hong Kong Institution of Civil Engineers, *Geotechnical Division*, 71-78.
- Fan, R.L., Zhang, L.M., Wang, H.J., and Fan, X.M. (2018). Evolution of debris flow activities in Gaojiagou Ravine during 2008–2016 after the Wenchuan earthquake. *Engineering Geology*, 235, 1-10.
- Ghorbanzadeh, O., Blaschke, T., Gholamnia, K., Meena, S.R., Tiede, D., and Aryal, J. (2019). Evaluation of different machine learning methods and deep-learning convolutional neural networks for landslide detection. *Remote Sensing*, 11(2), 196.
- Guzzetti, F., Mondini, A. C., Cardinali, M., Fiorucci, F., Santangelo, M., and Chang, K. T. (2012). Landslide inventory maps: New tools for an old problem. *Earth-Science Reviews*, 112(1-2), 42-66.
- Lei, T., Zhang, Y., Lv, Z., Li, S., Liu, S., and Nandi, A.K. (2019). Landslide inventory mapping from bitemporal images using deep convolutional neural networks. *IEEE Geoscience and Remote Sensing Letters*, 16(6), 982-986.
- Nichol, J., and Wong M.S. (2005). Detection and interpretation of landslides using satellite images. *Land Degradation & Development*, 16(3), 243-255.
- Ronneberger, O., Fischer, P., and Brox, T. (2015). U-net: Convolutional networks for biomedical image segmentation. *International Conference on Medical Image Computing and Computer-assisted Intervention*, 234-241.
- Su, Z., Chow, J.K., Tan, P.S., Wu, J., Ho, Y.K., and Wang, Y.H. (2021). Deep convolutional neural network-based pixel-wise landslide inventory mapping. *Landslides*, 18(4), 1421-1443.
- Wang, H. J. (2020). Machine learning powered natural terrain landslide identification and susceptibility assessment. PhD Thesis, *The Hong Kong University of Science and Technology*, Hong Kong.
- Xiao, T., Zhang, L.M., Cheung, R.W.M., and Lacasse, S. (2022). Predicting spatio-temporal man-made slope failures induced by rainfall in Hong Kong using machine learning techniques. *Géotechnique*, 1-17. DOI: 10.1680/jgeot.21.00160
- Zhang, P., Xu, C., Ma, S., Shao, X., Tian, Y., and Wen, B. (2020). Automatic extraction of seismic landslides in large areas with complex environments based on deep learning: an example of the 2018 Ibuli Earthquake, Japan. *Remote Sensing*, 12(23), 3992.
- Zhang, Y., and Rakesh K.M. (2012). A review and comparison of commercially available pan-sharpening techniques for high-resolution satellite image fusion. *IEEE International Geoscience and Remote Sensing Symposium*, 182-185.